Geophysical Research Letters

RESEARCH LETTER
10.1029/2019GL085728

Lipid Biomarkers Quantify Holocene Summer Temperature and Ice Cap Sensitivity in Icelandic Lakes

David J. Harning[1,2], Lorelei Curtin[3], Áslaug Geirsdóttir[1], William J. D'Andrea[3], Gifford H. Miller[2], and Julio Sepúlveda[2]

[1]Faculty of Earth Sciences, University of Iceland, Reykjavik, Iceland, [2]Institute of Arctic and Alpine Research and Department of Geological Sciences, University of Colorado Boulder, Boulder, CO, USA, [3]Lamont-Doherty Earth Observatory, Columbia University, New York, New York, USA

Key Points:
- We developed a downcore alkenone U^{K}_{37}-brGDGT temperature cross-calibration for lake sediment in Iceland
- Our empirical reconstruction is the first terrestrial record to reliably quantify Holocene summer temperature in Iceland
- Coupled with firm Holocene ice cap reconstructions and IPCC emission scenarios, the Drangajökull ice cap could disappear by 2050 CE

Supporting Information:
- Supporting Information S1

Correspondence to:
D. J. Harning,
david.harning@colorado.edu

Citation:
Harning, D. J., Curtin, L., Geirsdóttir, Á., D'Andrea, W. J., Miller, G. H., & Sepúlveda, J. (2020). Lipid biomarkers quantify Holocene summer temperature and ice cap sensitivity in Icelandic lakes. *Geophysical Research Letters*, *47*, e2019GL085728. https://doi.org/10.1029/2019GL085728

Received 7 OCT 2019
Accepted 15 JAN 2020
Accepted article online 21 JAN 2020
Corrected 2 MAR 2020

This article was corrected on 2 MAR 2020. See the end of the full text for details.

Abstract Although recent research has made significant advances in characterizing Iceland's Holocene environmental history, the region still lacks reliable and continuous records of corresponding paleotemperature. Here we merge bacterial and algal lipid biomarkers (branched glycerol dialkyl glycerol tetraethers and long-chain alkenones, respectively) to quantify Holocene temperature change from a small lake in northwest Iceland. Our local proxy record shows that early Holocene and late Holocene temperatures ranged from 3.2 to −1.1 °C relative today, which are in close agreement with independent estimates from regional ice cap models. At 2.4 ka, we observe abrupt cooling across bacteria-, algae-, and glacier-derived proxy records, which may have been initiated by extratropical volcanism and/or ocean/atmospheric climate variability of the North Atlantic region. Using early Holocene warmth and ice cap demise as an analog for modern climate change, Intergovernmental Panel on Climate Change temperature projections suggest that the local ice cap, Drangajökull, could vanish by ~2050 CE.

Plain Language Summary Numerical climate and glacier models are necessary tools to forecast the changing climate of the coming century. However, in order to improve the accuracy and precision of the models, it is critical to test their ability to reconstruct past climate observed through proxy records. Here, we present an Icelandic lake temperature proxy record for the last 10,000 years that covers a period in Earth's history when temperatures were comparable to those expected in our near future. This proxy temperature reconstruction is used to assess the controls on Iceland's climate, the performance of existing Icelandic glacial models and, alongside regional climate simulations, forecast the future demise of a local ice cap. We find that Iceland's past temperatures are strongly controlled by regional atmospheric and oceanic variability, and that as modern temperatures continue to rise, a local ice cap in northwest Iceland may vanish by 2050 CE. This forecast holds critical value for Icelandic policy making and energy security, as hydroelectric dams on glacier-fed rivers currently provide ~73% of Iceland's electricity.

1. Introduction

Iceland's position at the confluence of major North Atlantic oceanic currents integral to global heat distribution (Figure 1a, Wunsch, 1980) make it a strategic location to improve our understanding of the Northern Hemisphere climate system. A combination of proxy and modeling datasets demonstrates that during the last deglaciation, residual ice caps disappeared between 10.3 and 9.2 ka before present (BP), and that the warmest Holocene temperatures were reached during the Holocene thermal maximum (HTM, 7.9–5.5 ka BP) (Flowers et al., 2008; Geirsdóttir, Miller, Axford, & Ólafsdóttir, 2009, 2013, 2019; Larsen et al., 2012; Anderson et al., 2018; Harning, Geirsdóttir, Miller, & Zalzal, 2016; Harning, Thordarson, et al., 2018). Subsequent to peak warmth, high-resolution Icelandic climate reconstructions reflect long-term cooling and ice cap expansion driven principally by variations in Earth's orbit and the concomitant decline in Northern Hemisphere summer insolation (Larsen et al., 2012; Geirsdóttir et al., 2013, 2019; Harning, Geirsdóttir, & Miller, 2018), with the lowest temperatures and largest ice cap dimensions achieved during the Little Ice Age (LIA, 1250–1850 CE) (Flowers et al., 2008; Larsen et al., 2011; Harning, Geirsdóttir,

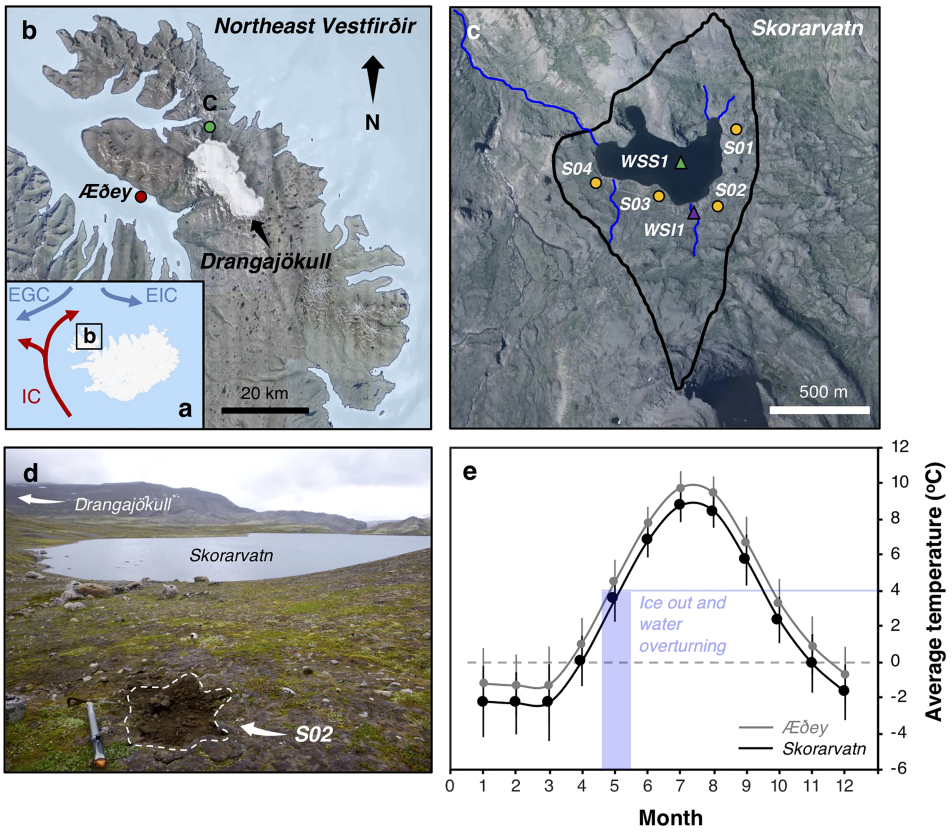

Figure 1. Overview of study location. (a) Iceland with simplified ocean surface currents. Red = warm, Atlantic currents and blue = cool, Arctic currents. (b) Northeastern Vestfirðir peninsula showing the local ice cap, Drangajökull, and local weather station, Æðey. (c) Skorarvatn and its catchment (black), river inlets/outlets (blue), soil sampling sites (yellow), and water sampling sites (purple and green). 2005 base imagery courtesy of Loftmyndir ehf. (d) Example of shallow catchment soil site (S02). (e) 1954–2011 CE average monthly temperature and standard deviation from Æðey (gray, IMO, 2012) and lapse rate adjusted temperature for Skorarvatn (black, 0.6 ^{o}C/100 m).

Miller, & Anderson, 2016; Anderson et al., 2018). However, these reconstructions predominately rely on qualitative studies, which limit our ability to assess the rate and magnitude of Iceland's Holocene climate variability.

The few quantitative Holocene temperature records that exist from Iceland are derived from subfossil chironomid assemblages (Diptera: Chironomidae, or non-biting midges, Caseldine et al., 2003; Axford et al., 2007; Langdon et al., 2010). However, Icelandic chironomid communities are also influenced by the carbon content of lake sediment (Langdon et al., 2008) and post-settlement soil erosion (Lawson et al., 2007), are hampered by limited taxonomic resolution, and are ill-suited for large, deep lakes (Axford et al., 2009). Consequently, chironomid-based temperature reconstructions in Iceland have proven to be challenging (Holmes et al., 2016) as they do not conform to Iceland's known qualitative Holocene climate history. Glacier modeling studies have estimated the magnitude of temperature difference between the HTM and the LIA (ΔT = 3.1–5.5 ^{o}C, Flowers et al., 2008; Anderson et al., 2018), but these are not continuous and do not capture the centennial-scale perturbations evident in the Holocene lake records (Larsen et al., 2012; Geirsdóttir et al., 2013, 2019; Harning, Geirsdóttir, & Miller, 2018).

Recent advances in the field of organic geochemistry have yielded a new set of tools for quantifying past temperature variability from a variety of sediment archives. Some of these, such as the methylation and cyclization of bacterial branched glycerol dialkyl glycerol tetraethers (brGDGTs), have previously been used to reconstruct mean annual air temperature from fjord sediments in northwest Iceland (Moossen et al., 2015). Although the Holocene trends look promising for brGDGT application in Iceland (Moossen et al., 2015), the existing fjord record is complicated by unconstrained sources of microbial production (i.e., sediment, water column, and/or soil), variable transport times between terrestrial and

marine brGDGTs, as well as bioturbation. Furthermore, the fjord record preceded recent analytical improvements that remove the influence of pH-sensitive brGDGT isomers (De Jonge et al., 2014; Hopmans et al., 2016). Other lipid-based paleothermometers, such as the degree of algal alkenone unsaturation, have proven effective for reconstructing past lake temperatures elsewhere in the Arctic (D'Andrea et al., 2011, 2012, 2016; Longo et al., 2016, 2018; van der Bilt et al., 2018). However, despite their potential, alkenone-based temperature reconstructions have not yet been reported from Icelandic lakes.

Here we merge brGDGT and alkenone paleothermometers to quantify Holocene temperature from a continuous lake sediment record in northwest Iceland (Skorarvatn, Figures 1a–1c). In addition, we analyze brGDGTs in catchment soil and lake water filtrate samples to test whether downcore brGDGTs have been dominated by in situ lake production. Given the lack of a regional brGDGT lake calibration, we use the established lake temperature relationship of alkenone unsaturation (Sun et al., 2007; Theroux et al., 2013; Toney et al., 2012) to locally cross-calibrate our high-resolution brGDGT record. The strong similarity between brGDGT-based temperatures and trends observed in qualitative climate proxies from the same lake (Harning, Geirsdóttir, & Miller, 2018) as well as the magnitude of Holocene temperature derived from theoretical glacier models (Anderson et al., 2018) underpins the fidelity of our novel paleotemperature record. Collectively, these strengths enable us to evaluate past and future climate and glacier sensitivity in Iceland.

2. Materials and Methods

Skorarvatn (183 m asl, 66.25627°N, 22.32213°W) is a small (192 m^2), non-glacial and dimictic lake located ~3-km north of the Drangajökull ice cap in northwest Iceland (Figures 1b and 1c) and at the intersection of warm, saline Atlantic currents and cool, sea-ice bearing Arctic currents (Figure 1a). The combination of isothermal water column temperatures in August 2016 (Table S1) and massive organic sediment composition (i.e. nonlaminated and bioturbated, Harning, Geirsdóttir, & Miller, 2018) suggests that the lake has likely remained oxic throughout most of the year. The catchment area is small (1.24 km^2) with sparse and discontinuous soil (brown andosol) accumulation reaching ~20-cm maximum depth. Vegetation is dominated by a variety of moss species, which tend to clump on isolated soil patches. A 2.5-m-long lake sediment core was collected in winter 2014 using a percussion-driven piston corer from the lake-ice platform (Harning, Geirsdóttir, Miller, & Anderson, 2016; Harning, Geirsdóttir, Miller, & Zalzal, 2016), and modern soil and water samples were collected in summer 2016 (Supporting Information S1). The lake sediment record relies on a combination of radiocarbon-dated macrofossils ($n = 7$) and regional marker tephra layers ($n = 5$) for age control (Harning, Thordarson, et al., 2018; Harning, Thordarson, et al., 2019) and has existing qualitative proxy records of high-resolution paleoclimate over the last ~10 ka (Harning, Geirsdóttir, & Miller, 2018). To quantify corresponding paleotemperature, we generated centennial-scale bacterial brGDGT and alkenone U^K_{37} records from Skorarvatn's downcore lake sediment record using established extraction and instrumental procedures (Data S2, Bligh & Dyer, 1959; Harning et al., 2019; Huguet et al., 2006; Longo et al., 2013; Hopmans et al., 2016; Wörmer et al., 2015).

3. Source Discrimination of brGDGTs

BrGDGTs are bacterial cell membrane lipids, which are ubiquitous in nature and preserved in geologic archives such as soil and lake sediment (Blaga et al., 2009; De Jonge et al., 2014; Foster et al., 2016; Pearson et al., 2011; Weijers et al., 2007). Although the biological source organism for brGDGTs remains speculative (Weijers et al., 2009), a variety of empirical studies have demonstrated a link between the degree of brGDGT methylation and air temperature in soil bacteria (Weijers et al., 2007; De Jonge et al., 2014; Naafs, Gallego-Sala, et al., 2017). In lake sediment records, the biological source of brGDGTs and interpretations of their reconstructed temperature is more complex. Lake sediment brGDGTs can originate from a combination of soil, water column, and/or surface sediment bacteria that may each respond to their own niche environmental conditions (Blaga et al., 2009; Colcord et al., 2017; Feng et al., 2019; Naeher et al., 2014; Russell et al., 2018; Weber et al., 2015, 2018). To help reduce some of this complexity, end-member sources can often be differentiated by the fractional abundances of individual brGDGTs (Martin et al., 2019; Niemann et al., 2012). Furthermore, proxies derived from archaeal isoprenoid GDGTs can help determine various redox

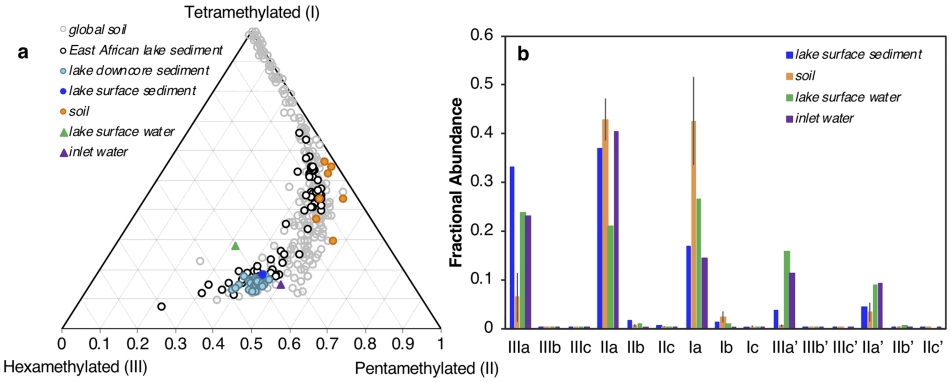

Figure 2. Bacterial branched glycerol dialkyl glycerol tetraethers (brGDGT) fractional abundances for Skorarvatn lake sediment ($n = 31$), soil ($n = 7$), lake surface water ($n = 1$), and inlet water ($n = 1$). (a) Total tetra-, penta-, and hexamethylated brGDGTs in comparison to global soil dataset ($n = 239$, De Jonge et al., 2014) and East African lake sediment ($n = 65$, Russell et al., 2018), and (b) individual brGDGT in Skorarvatn endmembers.

states of the lake water column (Blaga et al., 2009; Naeher et al., 2014) that may lead to changes in brGDGT production depth (i.e. surface vs bottom, Weber et al., 2018).

To help constrain brGDGT sources to the lake sediment record, we analyzed brGDGT distributions in catchment soils ($n = 7$, Data S1 and S3 and Figure S1) and water samples taken from the central surface portion of the lake ($n = 1$) and the main inlet ($n = 1$) (Figures 1c and 1d). When compared against the distribution of brGDGTs in global soils and lakes sediments, our data show a clear differentiation of brGDGT end-member populations between soil and aquatic sources (Figure 2). Lake sediment samples, as well as water filtrate samples, are dominated by hexa- and pentamethylated brGDGTs with minor contributions from tetramethylated brGDGT, while soils are dominated by penta- and tetramethylated brGDGTs (Figure 2a). Both the lake and inlet water samples feature higher relative abundances of 6-methyl brGDGT isomers compared to the lake sediment and soils (Figure 2b). Collectively, end-member brGDGT distributions suggest that for Skorarvatn, brGDGTs archived in its Holocene lake sediment record are not derived from the surrounding soils but have been dominated by in situ lake production. However, values of the isoprenoid GDGT-0/crenarchaeol ratio hint at the occurrence of archaeal methanogens and, thus, periodic bottom water anoxia during the early Holocene (Figure S3d, e.g. Blaga et al., 2009; Naeher et al., 2014). If the latter were the case, the depth habitat of brGDGT-producing bacteria may have possibly shifted to bottom waters at this time and, hence, may record deeper water column temperatures (Weber et al., 2018). Furthermore, we cannot rule out the occurrence of changes in the bacterial community associated with low oxygen conditions at this time that may have impacted the distribution of brGDGTs (e.g. Weber et al., 2018). Although brGDGT distributions from settling particles are consistent with the lower temperatures of the deeper water column in Swiss lakes (Weber et al., 2018), the combined effects of these factors on the distribution of brGDGTs in the environment remain largely unknown.

4. brGDGT Lake Temperature Calibrations

We explored the several existing lake temperature calibrations that separate 5- and 6-methyl brGDGT isomers for our downcore lake sediment record (Feng et al., 2019; Russell et al., 2018). Although the range of reconstructed temperatures spans ~14 ^{o}C (Figure S3a), we assume that each calibration should at least reflect relative mean summer air temperature (MSAT) due to Skorarvatn's de facto Arctic location that may shift brGDGT production to summer months as suggested for other high-latitude and -altitude regions (Deng et al., 2016; Peterse et al., 2014; Shanahan et al., 2013). As heterotrophic bacteria that synthesize brGDGTs do not require oxygen or light, we acknowledge that some winter production under ice cover is possible, which could result in an underestimation of MSAT. However, we favor a summer season interpretation given the empirical evidence from other cold regions until further in situ evidence from Iceland is available. From this, we argue that none of the existing calibrations yield realistic temperature histories for Iceland because of 1) consistent underestimation of sediment core top

reconstructed MSAT compared to the modern instrumental (Figure S3a) and 2) different temperature relationships of brGDGTs between Icelandic, African, and Chinese lakes. To demonstrate the latter point, we assessed the relationships among individual brGDGTs by computing a Pearson correlation coefficient matrix using the fractional abundances of each brGDGT and compared this against corresponding matrices from East Africa (Russell et al., 2018) and southwest China lakes (Feng et al., 2019) as well as global soil (De Jonge et al., 2014) and peat datasets (Naafs, Inglis, et al., 2017) (Figure S4). Skorarvatn's brGDGT relationships range from weakly positive to moderately negative, which in many cases are different from the sign and strength of brGDGT relationships from East Africa and southwest China lakes (Feng et al., 2019). Our main conclusion is that, depending on the region, the same brGDGT pairs can exhibit a strong positive correlation in one dataset and a negative correlation in another, which may result from a varying proportion of soil- versus lake-derived brGDGTs, site-specific environmental factors at each location, and/or the dominance of different microbial communities (Feng et al., 2019; Foster et al., 2016; Russell et al., 2018). Collectively, this evidence suggests that a local calibration is needed to quantify temperature from Skorarvatn's brGDGT distributions.

5. Alkenone U^{K}_{37}-brGDGT Calibration

In high-latitude freshwater lakes long-chain alkenones are biosynthesized by Group I haptophyte algae (D'Andrea et al., 2006; Richter et al., 2019; Theroux et al., 2010) that bloom in the spring/summer season following lake ice out and water overturning (D'Andrea et al., 2011; Longo et al., 2016, 2018). The degree of unsaturation, expressed as the relative abundances of C_{37} di-, tri-, and tetra-unsaturated alkenones (U^{K}_{37}, Brassell et al., 1986), is dominantly controlled by temperature change in haptophyte culture experiments (Sun et al., 2007; Theroux et al., 2013; Toney et al., 2012). We analyzed alkenone distributions of each of the 31 downcore samples; however, adequate abundance and chromatographic separation were only achieved in 10 lake sediment samples (Figure S5a). The abundance of tri-unsaturated isomers, expressed as RIK_{37} values at 0.48–0.63 (Longo et al., 2018, Data S2 and Figure S5b), suggests that the alkenones in Skorarvatn were primarily, if not exclusively, produced by Group I haptophytes throughout the sediment record. The timing of inferred ice out and seasonal overturning of the water column in Skorarvatn during May/June (Figure 1e) indicates that algal blooms likely occur shortly thereafter, consistent with a summer temperature seasonality noted for other high-latitude alkenone temperature reconstructions from Greenland and Svalbard (D'Andrea et al., 2011, 2012).

Given the complications of existing brGDGT lake temperature calibrations, we developed a site-specific downcore U^{K}_{37}-brGDGT cross-calibration to capture local lake MSAT and minimize prediction error. A calibration based on the regression of U^{K}_{37} values against the MBT'_{5ME} index (De Jonge et al., 2014) was not successful due to the lack of slope in Skorarvatn's MBT'_{5ME} index ($m = 0.000001$, Figure S3b) or correlation with U^{K}_{37} values ($R^2 = 0.07$, $p < 0.0001$, Figure S5c). Therefore, we opted for a stepwise forward selection (SFS) approach to find the best model that predicts U^{K}_{37} values using multiple combinations of the brGDGTs that feature an $R^2 > 0.1$ (Figure S6). This method has been shown to significantly improve error statistics in brGDGT lake calibrations (Feng et al., 2019; Pearson et al., 2011; Russell et al., 2018). Our best model ($R^2 = 0.92$, $p < 0.001$) includes two key brGDGTs that are known to feature high correlations with temperature in other lake and soil systems (IIIa and Ia,De Jonge et al., 2014 ; Russell et al., 2018), as well as a 6-methyl isomer biosynthesized in the oxygenated water column of Swiss lakes (IIIa', Weber et al., 2018):

$$U^{K}_{37-SFS} = -0.1540*[IIIa] + 0.3538*[Ia] + 1.0016*[IIIa'] - 0.7537.$$

The strong correlation between IIIa' fractional abundance and U^{K}_{37} values ($R^2 = 0.86$, $p < 0.0001$, Figure S6) is interesting given that in global soil (De Jonge et al., 2014) and East African lake datasets (Russell et al., 2018), IIIa' shows no individual correlation with temperature. However, recent incubation experiments for lake brGDGTs (Martínez-Sosa & Tierney, 2019) in addition to the environmental samples from East Africa (Russell et al., 2018) demonstrate a positive correlation between the abundance of total 6-methyl brGDGT isomers and temperature. As the physiological response of brGDGT-producing bacteria is largely unknown, our results indicate that contrary to recent empirical datasets (De Jonge et al., 2014; Russell

et al., 2018), 6-methyl brGDGT isomers may be important in reconstructing past temperature in certain regions. Future work from local calibrations will help test whether this pattern is consistent across other Icelandic lakes, as well as better determine the specific seasonality of brGDGT production.

Downcore $U^{K}_{37\text{-SFS}}$ are converted to brGDGT MSAT using the established Group I haptophyte temperature calibration (D'Andrea et al., 2016):

$$U^{K}_{37} = 0.0287*T$$

and are reported relative to the sediment core top. Total standard error (1.3 °C) is propagated from the Group I haptophyte calibration (0.7 °C, D'Andrea et al., 2016) and our SFS model (0.4 °C).

6. Holocene Summer Temperature in Iceland

Our novel quantitative temperature reconstruction allows us to examine the timing, rate, and magnitude of northwest Iceland temperature variations during the Holocene, as well as the factors responsible for these changes. Moreover, we can also examine the veracity of theoretical modeling studies based on glacier reconstructions (Anderson et al., 2018) and the extent to which temperature has impacted other paleolimnological proxies from Skorarvatn (Harning, Geirsdóttir, Miller, & Anderson, 2016; Harning, Geirsdóttir, Miller, & Zalzal, 2016; Harning, Geirsdóttir, & Miller, 2018). This is of paramount importance as existing quantitative records, such as those derived from subfossil chironomid assemblages (Axford et al., 2007; Caseldine et al., 2003; Langdon et al., 2010), have shown marked inconsistencies with the trends observed in qualitative climate proxy datasets. Although BSi from lakes with high sedimentation rates has been correlated with spring/summer temperature over the instrumental period (Geirsdóttir, Miller, Thordarson, & Ólafsdóttir, 2009) and has been used to qualitatively constrain Holocene temperature trends in Iceland (Geirsdóttir et al., 2019), our lipid-based approach is the first to include a proxy (i.e. U^{K}_{37}) that has had independent evaluation of temperature sensitivity through algae culture experiments (Sun et al., 2007; Theroux et al., 2013; Toney et al., 2012).

During the early Holocene (11.7 to 8.2 ka BP), geologic evidence shows that remnants of the Icelandic ice sheet (i.e. proto-Drangajökull) retreated from Skorarvatn's catchment by ~9.3 ka BP (Harning, Geirsdóttir, & Miller, 2018) and likely disappeared shortly thereafter, by ~9.2 ka BP (Figure 3f, Harning, Geirsdóttir, Miller, & Zalzal, 2016). Subsequently, qualitative paleoclimate records from Skorarvatn suggest that peak diatom productivity (BSi, Figure 3c, Harning, Geirsdóttir, Miller, & Zalzal, 2016) and stabilization of soils within the catchment (low C/N and enriched bulk $\delta^{13}C$, Figures 3d and 3e, Harning, Geirsdóttir, & Miller, 2018) occurred between ~9.2 and 7.9 ka BP likely in response to high Northern Hemisphere summer insolation and the concomitant warmth (Figure 3a). Theoretical modeling simulations for Drangajökull, using regional ice core and marine temperature proxy records tuned to local instrumental datasets, require HTM temperatures 2.5 to 3 °C above the late 20th century average to match the geologic record (Anderson et al., 2018) (Figure 3b). Our brGDGT record is the first to independently confirm local early Holocene warmth in Iceland with MSAT up to 3.2 °C above modern (Figure 3b). The relatively lower brGDGT MSAT between 9.2 and 8.1 ka BP (average 2.0 °C above modern) compared to 7.6 ka BP (3.2 °C above modern) may result from a combination of effects. These include freshwater discharge events from the waning Laurentide ice sheet (e.g. 8.2 ka BP Event), prolonged atmospheric sulfate injection from northern hemisphere volcanic eruptions (see Geirsdóttir, Miller, Axford, & Ólafsdóttir, 2009, 2013; Larsen et al., 2012; Harning, Geirsdóttir, & Miller, 2018), and/or potentially altered redox conditions that may result in subdued bottom water temperature estimates. However, despite these potential climate/proxy modulators, our average early Holocene brGDGT MSAT of 2.2 °C above modern falls within the range of those based on the local glacier models (Anderson et al., 2018) (Figure 3b). The marked consistency between glacier models relying on regional proxy datasets and our independent brGDGT MSAT record provide firm evidence that the early Holocene demise of Drangajökull required summer temperatures at least 2.2 °C above modern.

The middle (8.2 to 4.2 ka BP) to late Holocene (4.2 ka BP to present) climate around Skorarvatn is characterized by local cooling, reflected by lower lake diatom productivity (Figure 3c, Harning, Geirsdóttir, Miller, & Anderson, 2016) and reduced catchment stability (Figures 3d and 3e, Harning, Geirsdóttir, & Miller, 2018).

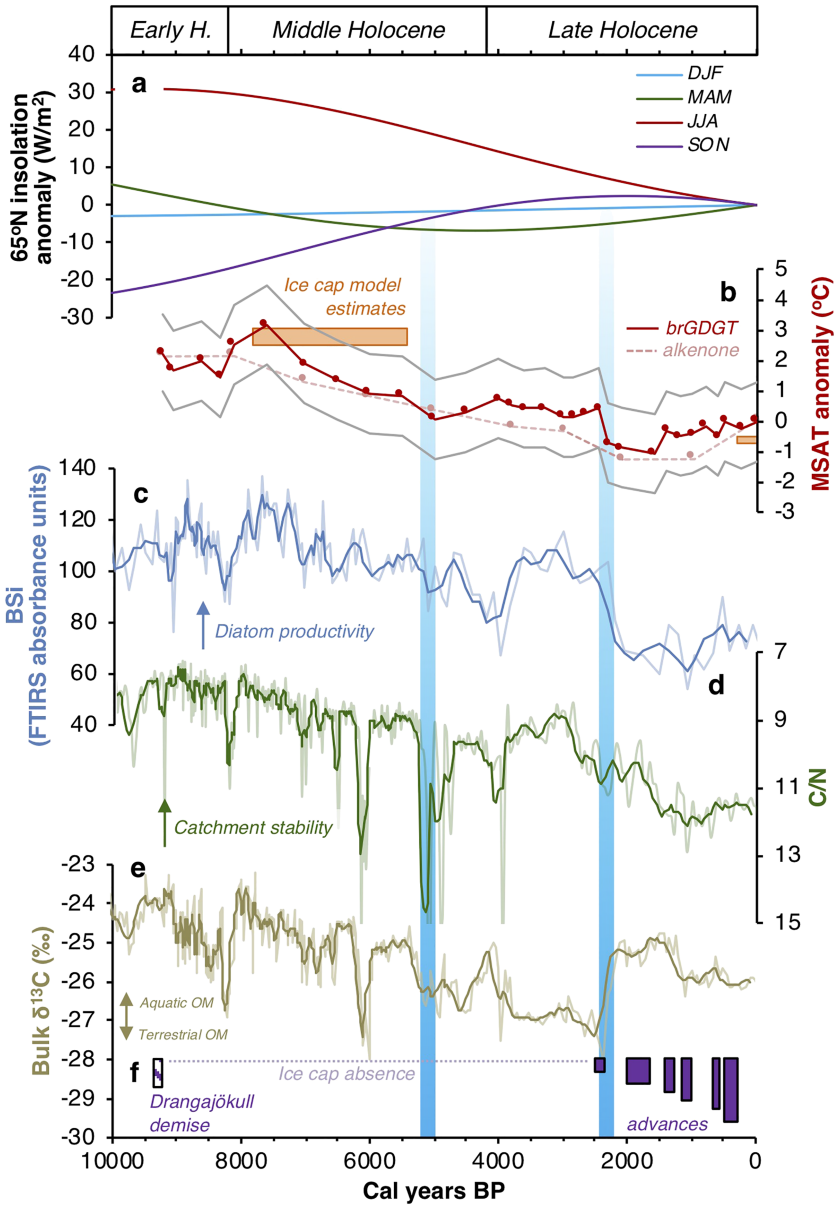

Figure 3. Comparison of local paleoclimate records. (a) Seasonal Northern Hemisphere insolation curves (Laskar et al., 2004), (b) MSAT anomalies from Skorarvatn lake sediment based on bacterial branched glycerol dialkyl glycerol tetraether $U^{K}_{37\text{-SFS}}$ model (bold red line) and original U^{K}_{37} values using the Group I haptophyte calibration (dash red line, D'Andrea et al., 2016). Propagated standard error for $U^{K}_{37\text{-SFS}}$ model is shown with gray lines. Orange boxes frame the classical timing (Geirsdóttir et al., 2013) and range of Holocene thermal maximum and Little Ice Age temperatures estimated from Drangajökull modeling (Anderson et al., 2018), (c) BSi record from Skorarvatn (Harning, Geirsdóttir, Miller, & Zalzal, 2016), (d) inverted C/N record from Skorarvatn (Harning, Geirsdóttir, & Miller, 2018), (e) bulk $\delta^{13}C$ record from Skorarvatn used as a proxy for changes in organic matter source (Harning, Geirsdóttir, & Miller, 2018) (f) timing of Drangajökull's early Holocene demise (hashed box, Harning, Geirsdóttir, Miller, & Zalzal, 2016) and late Holocene glacier advances (solid boxes) based on geologic datasets (Harning, Geirsdóttir, Miller, & Anderson, 2016, Harning, Geirsdóttir, & Miller, 2018). Taller boxes correspond to relatively larger glacier area. Panels c and d show 100-year running means in bold. Blue vertical bars highlight identified periods of cooling.

Consistent with an insolation forcing, brGDGT MSAT document first-order cooling from 3.2 above to 1.1 °C below modern (Figures 3a and 3b). Major stepwise brGDGT cooling events occur at 5.5 and 2.4 ka BP, which are two notable periods of local (Harning, Geirsdóttir, Miller, & Anderson, 2016; Harning, Geirsdóttir, & Miller, 2018) and regional cooling (Geirsdóttir et al., 2013, 2019; Larsen et al., 2012) expressed in Icelandic

paleoclimate and ice cap records. The cooling observed at 2.4 ka BP reflects the largest rate and magnitude of temperature variability in our brGDGT MSAT record (−1.2 °C, Figure 3b). Coeval changes in other local summer temperature-sensitive proxies (i.e. reduction in diatom productivity and the nucleation of the local ice cap, Figures 3c–3f, Harning, Geirsdóttir, Miller, & Anderson, 2016; Harning, Geirsdóttir, Miller, & Zalzal, 2016), point to temperature as the dominant control on brGDGT distributions at this time, with a relatively lower influence from other environmental and biological variables (De Jonge et al., 2019; Naeher et al., 2014; Weber et al., 2018). Given the limited change in Northern Hemisphere insolation values at 2.4 ka (Figure 3a, Laskar et al., 2004), other forcing mechanisms must be responsible for the abrupt change in local climate.

Beginning at ~2.8 ka BP, salinity changes in the Labrador Sea and south of Iceland indicate a weakening Atlantic meridional overturning circulation that reduced northward heat transport for several centuries (Thornalley et al., 2009). Superimposed on this oceanographic cooling was a large tropical eruption at 2.4 ka BP that resulted in the largest negative radiative forcing over the last several millennia (Sigl et al., 2015). In addition, a pronounced centennial-scale shift to the negative mode of the North Atlantic Oscillation (NAO), one of the leading modes of internal climate variability in the Northern Hemisphere, has been proposed at this time (Olsen et al., 2012). Although the NAO record may at times be intrinsically linked to Atlantic meridional overturning circulation variability, the atmospheric pressure differential associated with negative NAO pushes the prevailing westerlies southward, which then allows colder, northerly winds to dominate north of Iceland (Hurrell et al., 2003). Consequently, sea ice export to Iceland would then be expected to increase, as is observed in IP_{25} proxy records from the north Iceland shelf at 2.4 ka BP (Cabedo-Sanz et al., 2016). The close timing of regional climate changes with the cooling observed in northwest Iceland records point to two potential climate change triggers (volcanism and negative NAO) over background Atlantic meridional overturning circulation variability, with cooling sustained by sea ice feedbacks (e.g. Miller et al., 2012).

The LIA cold period occurred between 0.7 and 0.1 ka BP in Iceland, based on a combination of biological lake sediment proxy records (Geirsdóttir, Miller, Thordarson, & Ólafsdóttir, 2009, 2013, 2019; Larsen et al., 2012; Harning, Geirsdóttir, Miller, & Anderson, 2016; Harning, Geirsdóttir, & Miller, 2018) and ice cap reconstructions (Flowers et al., 2008; Larsen et al., 2011; Harning, Geirsdóttir, Miller, & Anderson, 2016; Anderson et al., 2018). A suite of lake sediment proxy records from west and central Iceland record severe soil erosion during the last several millennia that, in addition to human settlement, likely resulted from the deteriorating LIA climate (Geirsdóttir, Miller, Thordarson, & Ólafsdóttir, 2009, Geirsdóttir et al., 2013, 2019; Larsen et al., 2012). However, low C/N and enriched bulk $\delta^{13}C$ values in Skorarvatn lake sediment suggest limited mobilization of soil from the catchment to the lake at this time (Figures 3d and 3e, Harning, Geirsdóttir, Miller, & Anderson, 2016). The distinct clustering of lake sediment brGDGTs that are maintained throughout Skorarvatn's record (Figure 2) further supports this notion and, therefore, indicates that the delivery of soil-derived brGDGTs is not likely a confounding variable for our late Holocene brGDGT temperature record. Furthermore, the strong similarity of brGDGT MSAT with the independent record of local qualitative summer temperature (BSi) suggests that temperature remains the dominant control on brGDGT distributions through the LIA. At this time, brGDGT MSAT are in close agreement with those derived from the local theoretical glacier models that suggest summer temperatures were 0.6 to 0.8 °C below the late 20th century average (Figure 3b, Anderson et al., 2018), when Drangajökull achieved its largest Holocene dimensions (Figure 3f, Harning, Geirsdóttir, Miller, & Anderson, 2016).

7. Future Demise of the Local Ice Cap

Constraining the future status of Icelandic ice caps is critical for the country's energy security, as hydroelectric dams on glacier-fed rivers currently provide ~73% of Iceland's electricity (Orkumál, 2012). Since 1925 CE, reduced mass balance and retracted glacier lengths have been observed across Icelandic ice caps (Björnsson et al., 2013). Although some glaciers slowed in their retreat or advanced during the 1980s CE, instrumental data and glacier models indicate that the rate of summer warming, rather than the concomitant increase in precipitation, has continued to remain the primary control on their decadal-scale mass balance (Anderson et al., 2018, 2019; Björnsson et al., 2013). Glacier models show that Drangajökull's extent is particularly sensitive due to its low-relief, plateau topography, and that a 2 ^{o}C increase in air temperature over the late 20th century average could push its equilibrium line altitude (ELA) above the underlying

bedrock resulting in its rapid disappearance within ~50 years (Anderson et al., 2018). Building on this, a simplified ELA-glacier model projected the loss of accumulation area across 22 Icelandic glaciers under various emission scenarios, where Drangajökull's is likely lost within the next 50 years (Anderson et al., 2019). As no quantitative temperature record for Iceland existed at the time, these simulations relied on adjusted Holocene temperature forcings from regional marine and ice core proxy reconstructions to test their ability to reconstruct past and future glacier/ELA records. However, it is important to note that regional temperature records do not necessarily correlate to local terrestrial climate in a linear fashion.

To support previous glacier models, we provide observational constraint from our new local paleotemperature estimates. We make the assumption that when Drangajökull disappeared during the early Holocene, its ELA was above the highest local topography (e.g. Anderson et al., 2019). The corresponding average MSAT of 2.2 ^{o}C above modern, therefore, likely reflects minimum temperature required to achieve that ELA in the early Holocene, as well as in the future. Under this simplified scenario, Climate Model Intercomparison Project 5 ensemble mean summer air temperature projections for RCP 8.5 (highest emission scenario) above Iceland (IPCC, 2013) suggests that temperatures will reach 2.2 ^{o}C above modern by 2050 CE (Figure S7). If the Climate Model Intercomparison Project 5 multi-model uncertainty is considered, these temperatures may not be achieved until 2100 CE (Figure S7). Collectively, these data show that Drangajökull will likely lose its accumulation area within the next 30–70 years, which when achieved, will lead to rapid ice decay. Given that our conclusions echo those reached by glacier model sensitivity tests (Anderson et al., 2018, 2019), we have increased confidence in our projection. Although the strong agreement between lipid-based temperature constraint and ice cap simulations paints a somber picture for Drangajökull's future, the data indicate that there is still time for local governments to prepare accordingly.

Acknowledgments
The authors kindly thank West Tours (Ísafjörður) and Sydney Gunnarson for fieldwork support, Nadia Dildar and Nicole DeRoberts for laboratory assistance, and Lina Pérez-Angel for assistance with SFS model code. We appreciate feedback from two anonymous reviewers that greatly improve the overall quality and clarity of the manuscript. All data can be found online through NOAA's National Centers for Environmental Information database. This study has been supported by Columbia University's Chevron Student Initiative Fund, University of Iceland Research Fund, University of Colorado Boulder, and Icelandic Center for Research (RANNIS #163431051, 130775051, 141573052).

References

Anderson, L. S., Flowers, G. E., Jarosch, A. H., Aðalgeirsdóttir, G. T., Geirsdóttir, Á., Miller, G. H., et al. (2018). Holocene glacier and climate variations in Vestfirðir, Iceland, from the modeling of Drangajökull ice cap. *Quaternary Science Reviews*, *190*, 39–56.

Anderson, L. S., Geirsdóttir, Á., Flowers, G. E., Wickert, A. D., Aðalgeirsdóttir, G., & Thorsteinnsson, T. (2019). Controls on the lifespan of Icelandic ice caps. *Earth and Planetary Science Letters*, *527*, 11578.

Axford, Y., Geirsdóttir, Á., Miller, G. H., & Langdon, P. G. (2009). Climate of the Little Ice Age and the past 2000 years in northeast Iceland inferred from chironomids and other lake sediment proxies. *Journal of Paleolimnology*, *41*, 7–24.

Axford, Y., Miller, G. H., Geirsdóttir, Á., & Langdon, P. G. (2007). Holocene temperature history of northern Iceland inferred from subfossil midges. *Quaternary Science Reviews*, *26*, 3344–3358.

Björnsson, H., Pálsson, F., Gudmundsson, S., Magnússon, E., Adalgeirsdóttir, G., Jóhannesson, T., et al. (2013). Contribution of Icelandic ice caps to sea level rise: Trends and variability since the Little Ice Age. *Geophysical Research Letters*, *40*, 1546–1550.

Blaga, C. I., Reichart, G.-J., Heiri, O., & Sinninghe Damsté, J. S. (2009). Tetraether membrane lipid distribution in water-column particulate matter and sediments: A study from 47 European lakes along a north-south transect. *Journal of Paleolimnology*, *41*, 535–540.

Bligh, E. G., & Dyer, W. J. (1959). A rapid method of total lipid extraction and purification. *Canadian Journal of Biochemistry and Physiology*, *37*(8), 911–917. https://doi.org/10.1139/o59-099

Brassell, S. C., Eglington, G., Marlowe, I. T., Pflaumann, U., & Sarnthein, M. (1986). Molecular stratigraphy: A new tool for climatic assessment. *Nature*, *320*, 129–133.

Cabedo-Sanz, P., Belt, S. T., Jennings, A. E., Andrews, J. T., & Geirsdóttir, Á. (2016). Variability in drift ice export from the Arctic Ocean to the North Iceland shelf over the last 8000 years: A multi-proxy evaluation. *Quaternary Science Reviews*, *146*, 99–115.

Caseldine, C., Geirsdóttir, A., & Langdon, P. (2003). Efstadalsvatn—A multi-proxy study of a Holocene lacustrine sequence from NW Iceland. *Journal of Paleolimnology*, *30*, 55–73.

Colcord, D. E., Pearson, A., & Brassell, S. C. (2017). Carbon isotope composition of intact branched GDGT core lipids in Greenland lake sediments and soils. *Organic Geochemistry*, *110*, 25–32.

D'Andrea, W. J., Huang, Y., Fritz, S. C., & Anderson, N. J. (2011). Abrupt Holocene climate change as an important factor for human migration in West Greenland. *Proceedings of the National Academy of Sciences*, *108*, 9765–9769.

D'Andrea, W. J., Lage, M., Martiny, J. B. H., Laatsch, A. D., Amaral-Zettler, L. A., Sogin, M. L., & Huang, Y. (2006). Alkenone producers inferred from well-preserved 18S rDNA in Greenland lake sediments. *Journal of Geophysical Research*, *111*, G03013.

D'Andrea, W. J., Theroux, S., Bradley, R. S., & Huang, X. (2016). Does phylogeny control U^{k}_{37}-temperature sensitivity? Implications for lacustrine alkenone paleothermometry. *Geochimica et Cosmochimica Acta*, *175*, 168–180.

D'Andrea, W. J., Vaillencourt, D. A., Balascio, N. L., Werner, A., Roof, S. R., Retelle, M., & Bradley, R. S. (2012). Mild Little Ice Age and unprecedented recent warmth in an 1800 year lake sediment record from Svalbard. *Geology*, *40*, 1007–1010.

De Jonge, C., Hopmans, E. C., Zell, C. I., Kim, J.-H., Schouten, S., & Sinninghe Damsté, J. S. (2014). Occurrence and abundance of 6-methyl branched glycerol dialkyl glycerol tetraethers in soils: Implications for palaeoclimate reconstruction. *Geochimica et Cosmochimica Acta*, *141*, 97–112.

De Jonge, C., Radujkovic, R., Sigurdsson, B. D., Weedon, J. T., Janssens, I., & Peterse, F. (2019). Lipid biomarker temperature proxy responds to abrupt shift in the bacterial community composition in geothermally heated soils. *Organic Geochemistry*, *137*, 103897.

Deng, L., Jia, G., Jin, C., & Li, S. (2016). Warm season bias of branched GDGT temperature estimates causes underestimation of altitudinal lapse rate. *Organic Geochemistry*, *96*, 11–17.

Feng, X., Zhao, C., D'Andrea, W. J., Liang, J., Zhou, A., & Shen, J. (2019). Temperature fluctuations during the Common Era in subtropical southwestern China inferred from brGDGTs in a remote alpine lake. *Earth and Planetary Science Letters*, *510*, 26–36.

Flowers, G. E., Björnsson, H., Geirsdóttir, Á., Miller, G. H., Black, J. L., & Clarke, G. K. C. (2008). Holocene climate conditions and glacier variation in central Iceland from physical modelling and empirical evidence. *Quaternary Science Reviews*, *27*, 797–813.

Foster, L. C., Pearson, E. J., Juggins, S., Hodgson, D. A., Saunders, K. M., Verleyen, E., & Roberts, S. J. (2016). Development of a regional glycerol dialkyl glycerol tetraether (GDGT)-temperature calibration for Antarctic and sub-Antarctic lakes. *Earth and Planetary Science Letters*, *433*, 370–379.

Geirsdóttir, Á., Miller, G. H., Andrews, J. T., Harning, D. J., Anderson, L. S., Florian, C., et al. (2019). The onset of Neoglaciation in Iceland and the 4.2 ka event. *Climate of the Past*, *15*, 25–40.

Geirsdóttir, Á., Miller, G. H., Axford, Y., & Ólafsdóttir, S. (2009). Holocene and latest Pleistocene climate and glacier fluctuations in Iceland. *Quaternary Science Reviews*, *28*, 2107–2118.

Geirsdóttir, Á., Miller, G. H., Larsen, D. J., & Ólafsdóttir, S. (2013). Abrupt Holocene climate transitions in the northern North Atlantic region recorded by synchronized lacustrine records in Iceland. *Quaternary Science Reviews*, *70*, 48–62.

Geirsdóttir, Á., Miller, G. H., Thordarson, T., & Ólafsdóttir, S. (2009). A 2000 year record of climate variations reconstructed from Haukadalsvatn, West Iceland. *Journal of Paleolimnology*, *41*, 95–115.

Harning, D. J., Andrews, J. T., Belt, S. T., Cabedo-Sanz, P., Geirsdóttir, Á., Dildar, N., et al. (2019). Sea ice control on winter subsurface temperatures of the North Iceland shelf during the Little Ice Age: A TEX_{86} calibration case study. *Paleoceanography and Paleoclimatology*, *34*, 1006–1021.

Harning, D. J., Geirsdóttir, Á., & Miller, G. H. (2018). Punctuated Holocene climate of Vestfirðir, Iceland, linked to internal/external variables and oceanographic conditions. *Quaternary Science Reviews*, *189*, 31–42.

Harning, D. J., Geirsdóttir, Á., Miller, G. H., & Anderson, L. (2016). Episodic expansion of Drangajökull, Vestfirðir, Iceland, over the last 3 ka culminating in its maximum dimension during the Little Ice Age. *Quaternary Science Reviews*, *152*, 118–131.

Harning, D. J., Geirsdóttir, Á., Miller, G. H., & Zalzal, K. (2016). Early Holocene deglaciation of Drangajökull, Vestfirðir, Iceland. *Quaternary Science Reviews*, *153*, 192–198.

Harning, D. J., Thordarson, T., Geirsdóttir, Á., Ólafsdóttir, S., & Miller, G. H. (2019). Marker tephra in Haukadalsvatn lake sediment: A key to the Holocene tephra stratigraphy of northwest Iceland. *Quaternary Science Reviews*, *219*, 154–170.

Harning, D. J., Thordarson, T., Geirsdóttir, Á., Zalzal, K., & Miller, G. H. (2018). Provenance, stratigraphy and chronology of Holocene tephra from Vestfirðir, Iceland. *Quaternary Geochronology*, *46*, 59–76.

Holmes, N., Langdon, P. G., Caseldine, C. J., Wastegård, S., Leng, M. J., Croudace, I. W., & Davies, S. M. (2016). Climatic variability during the last millennium in Western Iceland from lake sediment records. *The Holocene*, *26*, 756–771.

Hopmans, E. C., Schouten, S., & Sinninghe Damsté, J. S. (2016). The effect of improved chromatography on GDGT-based palaeoproxies. *Organic Geochemistry*, *93*, 1–6.

Huguet, C., Hopmans, E. C., Febo-Ayala, W., Thompson, D. H., Sinninghe Damsté, J. S., & Schouten, S. (2006). An improved method to determine the absolute abundance of glycerol dibiphytanyl glycerol tetraether lipids. *Organic Geochemistry*, *37*, 1036–1041.

Hurrell, J. W., Kushnir, Y., Ottersen, G., & Visbeck, M. (2003). An overview of the North Atlantic oscillation. *Geophysical Monograph*, *134*, 1–35.

Icelandic Meteorological Office (2012). Climatological data. Available at: http://en.vedur.is/climatology/data/. (Accessed: 30th September 2019).

IPCC (2013). The Physical Science Basis. In T. F. Stocker, et al. (Eds.). *Contribution of Working Group I to the Fifth Assessment Report of the Intergovernmental Panel on Climate Change*. (1535 pp.). Cambridge, United Kingdom and New York, NY, USA: Cambridge University Press.

Langdon, P. G., Leng, M. J., Holmes, N., & Caseldine, C. J. (2008). Environmental controls on modern chironomid faunas from NW Iceland and implications for reconstructing climate change. *Journal of Paleolimnology*, *40*, 273–293.

Langdon, P. G., Leng, M. J., Holmes, N., & Caseldine, C. J. (2010). Lacustrine evidence of early-Holocene environmental change in northern Iceland: A multiproxy palaeoecology and stable isotope study. *The Holocene*, *20*, 205–214.

Larsen, D. J., Miller, G. H., Geirsdóttir, Á., & Ólafsdóttir, S. (2012). Non-linear Holocene climate evolution in the North Atlantic: A high-resolution, multi-proxy record of glacier activity and environmental change from Hvítárvatn, central Iceland. *Quaternary Science Reviews*, *39*, 14–25.

Larsen, D. J., Miller, G. H., Geirsdóttir, Á., & Thordarson, T. (2011). A 3000-year varved record of glacier activity and climate change from the proglacial lake Hvítárvatn, Iceland. *Quaternary Science Reviews*, *30*, 2715–2731.

Laskar, J., Robutel, P., Gastineau, M., Correia, A. C. M., & Levrard, B. (2004). A long-term numerical solution for the insolation quantities of the Earth. *Astronomy and Astrophysics*, *428*, 261–285.

Lawson, I. T., Gathorne-Hardy, F. J., Church, M. J., Newton, A. J., Edwards, K. J., Dugmore, A. J., & Einarsson, Á. (2007). Environmental impacts of the Norse settlement: Palaeoenvironmental data from Mývatnssveit, northern Iceland. *Boreas*, *36*, 1–19.

Longo, W. M., Huang, Y., Yao, Y., Zhao, J., Gilbin, A. E., Wang, X., et al. (2018). Widespread occurrence of distinct alkenones from Group I haptophytes in freshwater lakes: Implications for paleotemperature and paleoenvironmental reconstructions. *Earth and Planetary Science Letters*, *492*, 239–250.

Longo, W. M., Theroux, S., Gilbin, A. E., Zheng, Y., Dillon, J. T., & Huang, Y. (2016). Temperature calibration and phylogenetically distinct distributions for freshwater alkenones: Evidence from northern Alaskan lakes. *Geochimica et Cosmochimica Acta*, *180*, 177–196.

Longo, W. N., Dillon, J. T., Tarazo, R., Salacup, J. M., & Huang, T. (2013). Unprecedented separation of long chain alkenones from gas chromatography with a poly (trifluoropropylmethylsiloxane) stationary phase. *Organic Geochemistry*, *65*, 94–102.

Martin, C., Ménot, G., Thouveny, N., Davtian, N., Andrieu-Ponel, V., Reille, M., & Bard, E. (2019). Impact of human activites and vegetation changes on the tetraether sources in Lake St Front (Massif Central, France). *Organic Geochemistry*, *135*, 38–52.

Martínez-Sosa, P., & Tierney, J. (2019). Lacustrine brGDGT response to microcosm and mesocosm incubations. *Organic Geochemistry*, *127*, 12–22.

Miller, G. H., Geirsdóttir, Á., Zhong, Y., Larsen, D. J., Otto-Bliesner, B. L., Holland, M. M., et al. (2012). Abrupt onset of the Little Ice Age triggered by volcanism and sustained by sea-ice/ocean feedbacks. *Geophysical Research Letters*, *39*, 1–5.

Moossen, H., Bendle, J., Seki, O., Quillmann, U., & Kawamura, K. (2015). North Atlantic Holocene climate evolution recorded by high-resolution terrestrial and marine biomarker records. *Quaternary Science Reviews*, *129*, 111–127.

Naafs, B. D. A., Gallego-Sala, A. V., Inglis, G. N., & Pancost, R. D. (2017). Refining the global branched glycerol dialkyl glycerol tetraether (brGDGT) soil temperature calibration. *Organic Geochemistry*, *106*, 48–56.

Naafs, B. D. A., Inglis, G. N., Zheng, Y., Amesbury, M. J., Biester, H., Bindler, R., et al. (2017). Introducing global peat-specific temperature and pH calibrations based on brGDGT bacterial lipids. *Geochimica et Cosmochimica Acta*, *208*, 285–301.

Naeher, S., Peterse, F., Smittenberg, R. H., Niemann, H., Zigah, P. K., & Schubert, C. J. (2014). Sources of glycerol dialkyl glycerol tetraethers (GDGTs) in catchment soils, water column and sediments of Lake Rotsee (Switzerland)—Implications for the application of GDGT-based proxies for lakes. *Organic Geochemistry*, *66*, 164–173.

Niemann, H., Stadnitskaia, A., Wirth, S. B., Gilli, A., Anselmetti, F. S., Sinninghe Damsté, J. S., et al. (2012). Bacterial GDGTs in Holocene sediments and catchment soils of a high alpine lake: Application of the MBT/CBT-paleothermometer. *Climate of the Past*, *8*, 889–906.

Olsen, J., Anderson, N. J., & Knudsen, M. F. (2012). Variability of the North Atlantic oscillation over the past 5,200 years. *Nature Geosciences*, *5*, 1–14.

Orkumál (2012). Raforka (Orkustofnun).

Pearson, E. J., Juggins, S., Talbot, H. M., Weckström, J., Rosén, P., Ryves, D. B., et al. (2011). A lacustrine GDGT-temperature calibration from the Scandinavian Arctic to Antarctic: Renewed potential for the application of GDGT-paleothermometry in lakes. *Geochimica et Cosmochimica Acta*, *75*, 6225–6238.

Peterse, F., Vonk, J. E., Holmes, R. M., Giosan, L., Zimov, N., & Eglington, T. I. (2014). Branched glycerol dialkyl glycerol tetraethers in Arctic lake sediments: Sources and implications for paleothermometry at high latitudes. *Journal of Geophysical Research: Biogeosciences*, *119*, 1738–1754.

Richter, N., Longo, W. M., George, S., Shipunova, A., Huang, Y., & Amaral-Zettler, L. (2019). Phylogenetic diversity in freshwater-dwelling Isochrysidales haptophytes with implications for alkenone production. *Geobiology*, *17*, 272–280.

Russell, J. M., Hopmans, E. C., Loomis, S. E., Liang, J., & Sinninghe Damsté, J. S. (2018). Distributions of 5- and 6-methyl branched glycerol dialkyl glycerol tetraethers (brGDGTs) in East African lake sediment: Effects of temperature, pH, and new lacustrine paleotemperature calibrations. *Organic Geochemistry*, *117*, 56–69.

Shanahan, T. M., Hughen, K. A., & Van Mooy, B. A. S. (2013). Temperature sensitivity of branched and isoprenoid GDGTs in Arctic lakes. *Organic Geochemistry*, *64*, 119–128.

Sigl, M., Winstrup, M., McConnell, J. R., Welten, K. C., Plunkett, G., Ludlow, F., et al. (2015). Timing and climate forcing of volcanic eruptions for the past 2,500 years. *Nature*, *253*, 543–549.

Sun, Q., Chu, G. Q., Liu, G. X., Li, S., & Wang, X. H. (2007). Calibration of alkenone unsaturation index with growth temperature for a lacustrine species, *Chrysotila lamellosa* (Haptophyceae). *Organic Geochemistry*, *38*, 1226–1234.

Theroux, S., D'Andrea, W. J., Toney, J., Amaral-Zettler, L., & Huang, Y. (2010). Phylogenetic diversity and evolutionary relatedness of alkenone-producing haptophyte algae in lakes: Implications for continental paleotemperature reconstructions. *Earth and Planetary Science Letters*, *300*, 311–320.

Theroux, S., Toney, J., Amaral-Zettler, L., & Huang, Y. S. (2013). Production and temperature sensitivity of long chain alkenones in the cultured haptophyte *Pseudoisochrysis paradoxa*. *Organic Geochemistry*, *62*, 68–73.

Thornalley, D. J. R., Elderfield, H., & McCave, I. N. (2009). Holocene oscillations in temperature and salinity of the surface subpolar North Atlantic. *Nature*, *457*(7230), 711–714. https://doi.org/10.1038/nature07717

Toney, J., Theroux, S., Andersen, R. A., Coleman, A., Amaral-Zettler, L., & Huang, Y. (2012). Culturing of the first 37:4 predominant lacustrine haptophyte: Geochemical, biochemical, and genetic implications. *Geochimica et Cosmochimica Acta*, *78*, 51–64.

van der Bilt, W. G. M., D'Andrea, W. J., Bakke, J., Balascio, N. L., Werner, J. P., Gjerde, M., & Bradley, R. S. (2018). Alkenone-based reconstructions reveal four-phase Holocene temperature evolution for high Arctic Svalbard. *Quaternary Science Reviews*, *183*, 204–213.

Weber, Y., De Jonge, C., Rijpstra, I. C., Hopmans, E. C., Stadnitskaia, A., Schubert, C. J., et al. (2015). Identification and carbon isotope composition of a novel branched GDGT isomer in lake sediments: Evidence for lacustrine branched GDGT production. *Geochimica et Cosmochimica Acta*, *154*, 118–129.

Weber, Y., Sinninghe Damste, J. S., Zopfi, J., De Jonge, C., Gilli, A., Schubert, C. J., et al. (2018). Redox-dependent niche differentiation provides evidence for multiple bacterial sources of glycerol tetraether lipids in lakes. *Proceedings of the National Academy of Sciences*, *115*, 10926–10931.

Weijers, J. W. H., Panoto, E., van Bleijswijk, J., Schouten, S., Rijpstra, W. I. C., Balk, M., et al. (2009). Constraints on the biological source(s) of the orphan branched tetraether membrane lipids. *Geomicrobiology Journal*, *26*, 402–414.

Weijers, J. W. H., Schouten, S., van den Donker, J. C., Hopmans, E. C., & Sinninghe Damsté, J. S. (2007). Environmental controls on bacterial tetraether membrane lipid distribution in soils. *Geochimica et Cosmochimica Acta*, *71*, 703–713.

Wörmer, L., Lipp, J. S., & Hinrichs, K. U. (2015). Comprehensive analysis of microbial lipids in environmental samples through HPLC-MS protocols. In *Hydrocarbon and lipid microbiology*, (pp. 289–317). Berlin, Heidelberg: Springer.

Wunsch, C. (1980). Meridional heat flux of the North Atlantic Ocean. *Proceedings of the National Academy of Sciences*, *77*, 5043–5047.

Erratum

In the originally published version of this article, the affiliation "Organic Geochemistry Laboratory, University of Colorado Boulder, Boulder, CO, USA" was incorrectly listed. This error has since been corrected, and the present version may be considered the authoritative version of record.